Paper from: *Advanced Computational Methods in Heat Transfer*, B Sunden and CA Brebbia (Editors).
ISBN 1-85312-906-2

Numerical modelling of transport phenomena in the vicinity of a gas-liquid interface

Y.Y. Yan, C.R. Gentle & J.B. Hull
School of Engineering, The Nottingham Trent University, U.K.

Abstract

This paper reports the authors' recent research progress on numerical modelling of transport phenomena in the vicinity of a gas-liquid interface. A numerical procedure based on the velocity–pressure formulation combined with a finite-volume discretisation of the Navier-Stokes equations written in a non-orthogonal body-fitted coordinate (BFC) with moving mesh arrangements has been developed and employed. On this basis, the external viscous flow with heat and mass transfer at the surface of an inviscid gas bubble is studied and calculated. It has been simulated that both the flow and the concentration fields in the vicinity of the interface of the bubble change with Reynolds and Weber numbers and affect bubble deformation. To further study the transport phenomena on both sides of the interface, a novel calculating procedure incorporating a multi-block iteration and moving mesh has been proposed. By applying a zonal boundary uniqueness theory, the procedure has also been applied to simulate a liquid drop problem in which a liquid drop moves in an immiscible unbounded quiescent fluid. The flow fields in the vicinity of the interface (inside and around the interface) and the interfacial characteristics of the liquid drop are studied and simulated.

1 Introduction

Two-phase bubbly flows accompanying heat and mass transfer are involved in many engineering applications in the water treatment, metallurgical, pharmaceutical and chemical industries. Boiling and condensation processes in the power and nuclear industries are also related to the motion and heat transfer behaviour of bubbles and drops. Such heat and mass transfer and phase change processes are closely in relation to transport phenomena in the vicinity of gas-liquid interfaces. For example, in a chemical reactor involving gas-liquid

Paper from: *Advanced Computational Methods in Heat Transfer*, B Sunden and CA Brebbia (Editors).
ISBN 1-85312-906-2

reactions, the production capacity of the reactor depends not only on the local rate of reaction but also on the interfacial area and the concentration gradients in each phase. In flow boiling, the fields in the vicinity of sliding bubble interfaces often play important roles in heat transfer intensification.

With regard to the studies of transport phenomena in the vicinity of gas-liquid interface, a starting point of research is to simulate the phenomena in the vicinity of a gas bubble interface. Early studies of this were focused on analytical solutions of bubble dynamics in which a zero/one-dimensional analysis was carried out [1]. Only in the last thirty years have numerical investigations become possible and active. An inviscid flow over a bubble was studied by several researchers such as in [2-3], in which the bubble was treated as a rigid stress-free sphere, the fluid was assumed to be inviscid and ideal and the Navier-Stokes equations were actually simplified to Euler equations. A creeping axisymmetric viscous flow around a spherical bubble at a low Reynolds number (Re<<1) was considered in [4-5], in which the Navier-Stokes equations were treated as Stokes equations. Later, in [6-7], an unsteady axisymmetric flow around the free surface of a bubble was simulated.

At the Nottingham Trent University, numerical modelling has been carried out in recent years to study and simulate transport phenomena in the vicinity of a gas-liquid interface, in particular the interface of a gas bubble in a liquid. This includes studies of numerical methods, code development and numerical simulations. This paper introduces the authors' recent progress in numerical modelling.

2 Numerical method

Basic Equations and Assumptions

In order to solve transport equations to determine a gas bubble rising through a hot liquid and the heat and mass transfer at the bubble surface, the following assumptions have been made: (1) the gas-liquid interface is completely free of surfactant; (2) the flow fields are steady and axisymmetric; (3) the bulk liquid is an incompressible Newtonian fluid, its density and viscosity are sufficiently large compared with those of a gas; (4) the dynamic pressure and stresses at the gas-side of the interface are negligible compared with those on the liquid side. In the present modelling, a numerical method based on a velocity-pressure formulation combined with a finite-volume discretisation of the Navier-Stokes related equations written in a non-orthogonal body-fitted coordinate (BFC) is employed. Cartesian velocity components (u,v) are employed as dependent variables to calculate the flow around, and the heat and mass transfer at the surface of a gas bubble. In this approach, the conservation equation for a general dependent variable ϕ in a non-orthogonal coordinate system (ξ,η) is written in a general form as

$$\frac{1}{r}\frac{\partial}{\partial\xi}r\left[\rho U\phi-\frac{\Gamma}{J}\left(\alpha\frac{\partial\phi}{\partial\xi}-\beta\frac{\partial\phi}{\partial\eta}\right)\right]+\frac{1}{r}\frac{\partial}{\partial\eta}r\left[\rho V\phi-\frac{\Gamma}{J}\left(-\beta\frac{\partial\phi}{\partial\xi}+\gamma\frac{\partial\phi}{\partial\eta}\right)\right]=JS\ ; \quad (1)$$

Paper from: *Advanced Computational Methods in Heat Transfer*, B Sunden and CA Brebbia (Editors).
ISBN 1-85312-906-2

where

$$U = u\frac{\partial r}{\partial \eta} - v\frac{\partial x}{\partial \eta}, \qquad V = v\frac{\partial x}{\partial \xi} - u\frac{\partial r}{\partial \xi}, \qquad \alpha = \left(\frac{\partial x}{\partial \eta}\right)^2 + \left(\frac{\partial r}{\partial \eta}\right)^2,$$

$$\beta = \frac{\partial x}{\partial \xi}\frac{\partial x}{\partial \eta} + \frac{\partial r}{\partial \xi}\frac{\partial r}{\partial \eta}, \quad \gamma = \left(\frac{\partial x}{\partial \xi}\right)^2 + \left(\frac{\partial r}{\partial \xi}\right)^2, \text{ and } J = \frac{\partial x}{\partial \xi}\frac{\partial r}{\partial \eta} - \frac{\partial x}{\partial \eta}\frac{\partial r}{\partial \xi}.$$

In the above equations, $S(\xi, \eta)$ is the source of ϕ in (ξ, η) coordinates, U and V are contravariant velocity components; α, β and γ are metric tensors; J is the transformation Jacob number; and Γ represents diffusion coefficients.

Boundary Conditions

Boundary conditions for velocity u, temperature T, and concentration C, at the inlet of the domain are given as:

$$u = V_\infty, \quad T = T_\infty \text{ (for heat transfer)}, \quad C = C_\infty \text{ (for mass transfer)}. \tag{2}$$

The conditions at the outlet of the domain are set as:

$$\frac{\partial u}{\partial x} = 0, \quad \frac{\partial T}{\partial x} = 0, \quad \frac{\partial C}{\partial x} = 0, \quad \text{and} \quad v = 0. \tag{3}$$

In addition, the bubble surface is considered as a shear-free interface with a zero velocity normal to the surface, i.e.

$$\tau_{nt} = 0 \quad \text{and} \quad v_n = 0 \tag{4}$$

where τ_{nt} is the local stress component in which the subscript n is for normal and t for tangential directions; v_n is the velocity in the direction normal to the surface. Figure 1 shows the non-orthogonal BFC and grid generations.

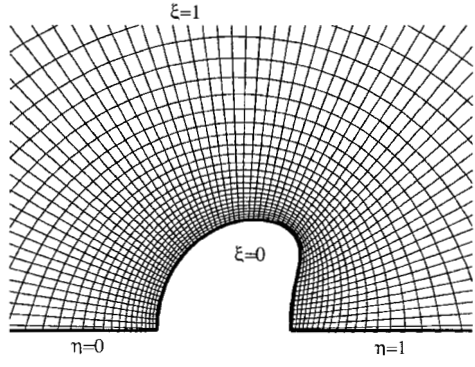

Figure 1 The non-orthogonal BFC and grid generation

Paper from: *Advanced Computational Methods in Heat Transfer*, B Sunden and CA Brebbia (Editors).
ISBN 1-85312-906-2

ADV Method for Treatment of Slip-Boundary Conditions

A method of alternating dependent variables (ADV) has been proposed by Li and Yan [8] where, for a bubble steadily rising through an incompressible liquid, the kinematic boundary condition was discussed, the gas-liquid interface was assumed to be free of surfactant and there was no mass flow across it. To impose slip-boundary conditions at such a free surface, a discretisation form of the velocities was expressed as:

$$u_b = u_{b-1} + \frac{\delta\eta}{\gamma_b}\left[\left(J - \frac{r_\xi}{x_\xi}\beta\right)_b \frac{\delta v}{\delta\xi} + \left(\frac{r_\xi}{x_\xi}\gamma\right)_b \frac{\delta v}{\delta\eta} - \left(\beta + \frac{r_\xi}{x_\xi}J\right)_b \frac{\delta u}{\delta\xi}\right] \tag{5}$$

and

$$v_b = u_b\left(\frac{r_\xi}{x_\xi}\right)_b; \tag{6}$$

where subscript b stands for values at the interface, b-1 denotes the values on the point of one grid away from the interface, and δ is a finite differential operator. A central differencing scheme is employed for the first derivation terms in ξ-direction, while a forward differencing scheme is used for the first derivation terms in η-direction. It can be seen from equations (5) and (6) that, a large slope of the bubble profile, such as $(\partial r/\partial x)_b = (r_\xi / x_\xi)_b = \infty$, could result in a numerical instability. Such instability is in particular obvious for ellipsoidal, spherical-cap and dimpled bubbles. To avoid this problem, alternating dependent variables (ADV) are derived from the boundary conditions and expressed as:

$$v_b = v_{b-1} + \frac{\delta\eta}{\gamma_b}\left[\left(\frac{x_\xi}{r_\xi}J - \beta\right)_b \frac{\delta v}{\delta\xi} + \left(\frac{x_\xi}{r_\xi}\gamma\right)_b \frac{\delta u}{\delta\eta} - \left(\frac{x_\xi}{r_\xi}\beta + J\right)_b \frac{\delta u}{\delta\xi}\right], \tag{7}$$

$$u_b = v_b\left(\frac{x_\xi}{r_\xi}\right)_b. \tag{8}$$

In the ADV method, equations (7) and (8) are used to calculate velocities v and u of the infinite slope at the segments, while equations (5) and (6) are employed to identify u and v in the vicinity of a zero slope at the segments. Using this method, flow with heat and mass transfer around a non-spherical, in particular a large curvature, bubble, is simulated.

The Direct-Predictor Method

A direct-predictor method was developed by Li & Yan [9] to predict the steady terminal shape of a rising bubble through a quiescent liquid, in which local imbalance of total normal stress is used to make improved predictions of the bubble interface position by means of an iteration approach.

To obtain an improved estimation of the bubble shape, a local excess of the total normal stresses can be considered as a force difference. This takes into

Paper from: *Advanced Computational Methods in Heat Transfer*, B Sunden and CA Brebbia (Editors).
ISBN 1-85312-906-2

account the pressure difference between inside and outside of a bubble, the difference in normal viscosity stresses and the difference in surface tension forces. It can be expressed as

$$\Delta P = p_0 - p + \frac{2}{\gamma J \,\mathrm{Re}}\left[\gamma\frac{\partial V}{\partial \eta} - \beta\frac{\partial V}{\partial \xi}\right] - \frac{1}{We\sqrt{\gamma}}\left(-\frac{x_\xi r_{\xi\xi} - r_\xi x_{\xi\xi}}{\gamma} + \frac{1}{r}\right). \tag{9}$$

This pressure difference is a kind of imbalanced normal force. It is this difference that results in a local displacement of the interface in the normal direction. The magnitude of the local displacement is proportional to the pressure difference.

This direct-predictor method is introduced to determine the improved shape of interface in a non-orthogonal BFC. This includes two stages of work. One is a predictor stage, in which new positions of the interface are directly predicted on the basis of the imbalance force at the interface at the last step of iteration. The other is the correction stage, in which the position is corrected using a condition of constant volume. Once new predictive positions have been determined, the exact positions are modified by a ratio of old volume to new volume. The new positions of the interface are expressed as:

$$x_b^p = x_b^n - C_b \Delta P \frac{(r_\xi)_b}{\sqrt{\gamma_b}} \text{ and } r_b^p = r_b^n + C_b \Delta P \frac{(x_\xi)_b}{\sqrt{\gamma_b}}. \tag{10}$$

The volume of the bubble is specified by

$$V = \int \pi r^2 \frac{\partial x}{\partial \xi} d\xi. \tag{11}$$

And the ratio of old volume to new volume is given by

$$\Re = \left(\frac{V^{old}}{V^{new}}\right)^{\frac{1}{3}}. \tag{12}$$

Based on the value (x_b^p, r_b^p) determined in the predictor stage, the positions of the interface are corrected by $\Re$ as:

$$x_b^{n+1} = \Re x_b^p \text{ and } r_b^{n+1} = \Re r_b^p. \tag{13}$$

The Zonal Boundary

To consider the fluid flow and heat and mass transfer on both sides of the interface, a novel calculation procedure has been developed by Yan, et al. to deal with multi-block iterations to ensure the uniqueness of the zonal boundary and an appropriate interpolation to calculate boundary values [10].

The zone boundary is defined as a boundary of the two blocks, as shown in Figure 2. In order to ensure the uniqueness of the boundary, the nodes of Block 1, where the mesh has been generated first, are employed to interpolate the boundary nodes of Block 2 using a cubic spline interpolation. The topology of

the near boundary cells is retained as a "general" quadrilateral with curvilinear sections as the boundaries. To calculate the area of the cell, a cubic spline fit is used to evaluate the determinant of the metric tensor, J; while the cell area is calculated as $J\Delta\xi^1\Delta\xi^2$ (1 & 2 is for inside and outside, respectively). This has been discussed and validated in detail in a recent paper [10].

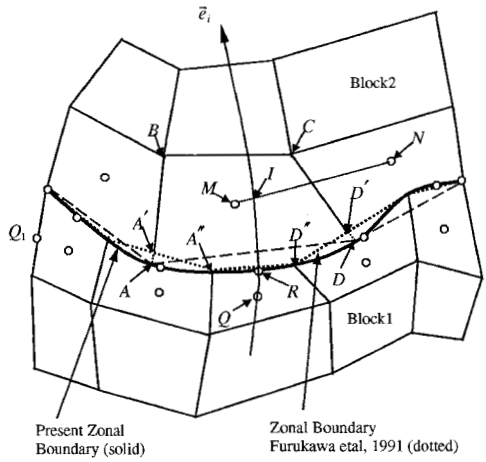

Figure 2 Multi-block and zonal boundary

3 Numerical results and discussion

Based on the numerical method described above, the flow and heat and mass transfer at the surface of a spherical gas bubble have been calculated by Yan and Li [11]. In that paper, distinguishable differences in both the flow fields and concentration (or temperature) distributions around a spherical bubble and the same scale rigid sphere have been simulated.

For a non-spherical bubble, the bubble rising at different Reynolds and Weber numbers defined on the basis of an equivalent diameter, $d_e = \sqrt[3]{6V_b/\pi}$, has been simulated. Figure 3 shows streamlines around the bubble. It can be seen that a flow separation at the rear of the bubble depends on *Re* and *We* numbers. At a high *We*, inertia forces on the bubble interface are larger than surface tension forces, so the bubble experiences a larger deformation. Such a deformation results in the bubble becoming either fore-flattened at a high Reynolds number or aft-flattened at a low Reynolds number. Furthermore, the geometric change of the bubble induces a change and accumulation of vorticity at the interface, and the vorticity accumulation is then brought to the rear area of the bubble by convection so as to form a flow re-circulation.

Figure 4 shows the concentration (or temperature) contours around a non-spherical bubble. Since convective heat and mass transfer strongly depends on the flow characteristics, the rate of the transfer across the bubble interface is in relation to the magnitude of *Re* and *We*. It can be seen from Figure 4 that, at a

Paper from: *Advanced Computational Methods in Heat Transfer*, B Sunden and CA Brebbia (Editors).
ISBN 1-85312-906-2

low *Re*, the concentration (or temperature) contours are almost uniformly distributed in all directions around the bubble, because the effect of convection is not as significant as mass or thermal diffusions. However, at a high *Re*, a flow separation appears at the rear of the bubble and concentration (or temperature) distributions become increasingly asymmetric. In fact, increasing Reynolds number gives an enhancement of convection so that the mass gets a chance to be transported into the rear of the bubbles. As a result of this, a region with a high concentration or high temperature is formed at the rear of bubbles.

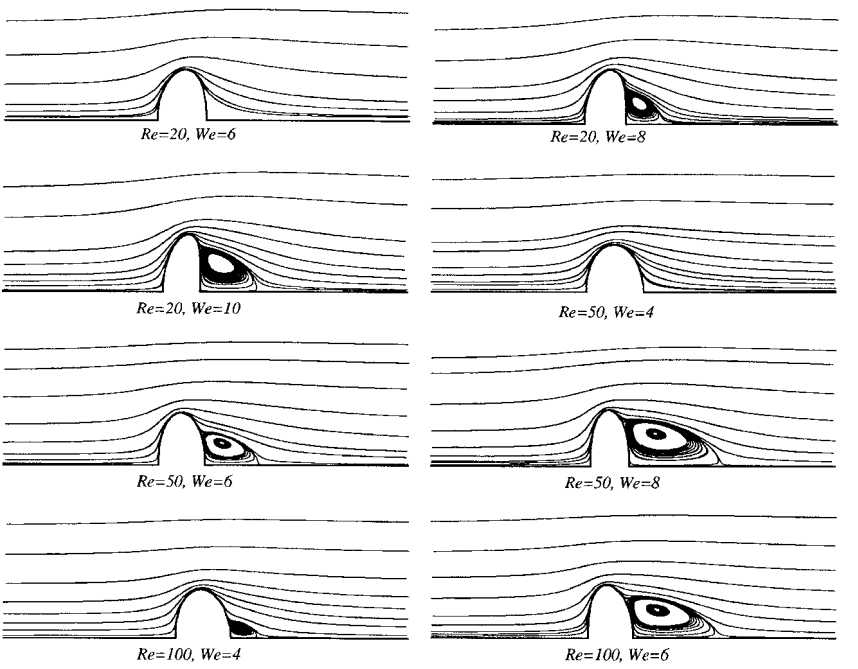

Figure 3 Streamlines for flow past an inviscid non-spherical

The evolution of bubble shape at different Reynolds numbers has been simulated based on the ADV and the direct predictor methods. Fig. 5 shows one example at Re=5. It is seen that at a low *We*, the bubble shape is nearly spherical. With a gradual increase of *We*, an evolution of bubble shape takes place from spherical to ellipsoidal, ellipsoidal-cap or more complicated nearly skirted. From the normal force balance point of view, a high *We* means that surface tension is small, so that the dominant force acting on the interface is a resultant force of viscous resistance and hydrostatic pressure. This resultant force results in a large deformation for the bubble. As the surface tension forces always try to maintain the original shape of the bubble, hydrostatic pressure and viscous forces are the dominant factor for a large deformation of the bubble.

Paper from: *Advanced Computational Methods in Heat Transfer*, B Sunden and CA Brebbia (Editors).
ISBN 1-85312-906-2

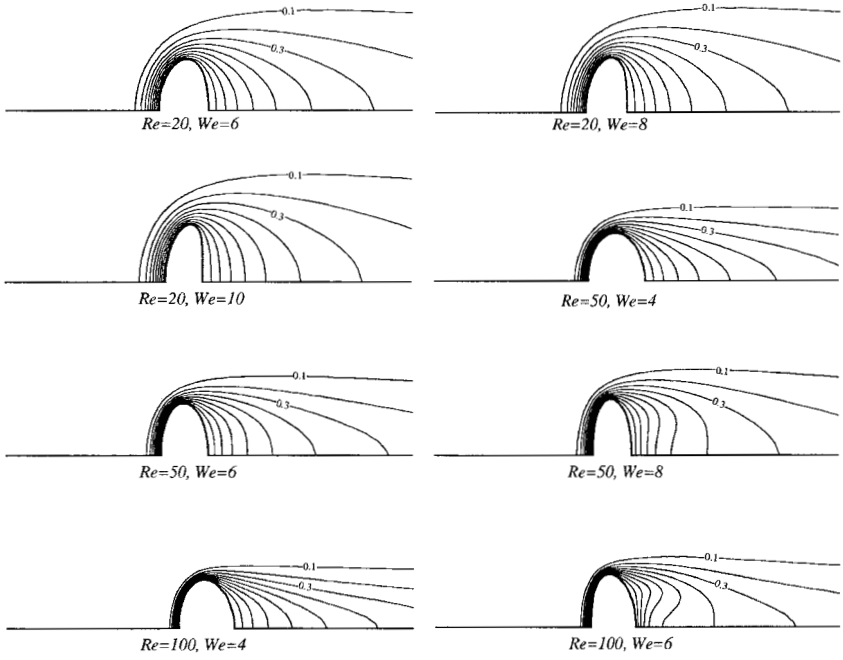

Figure 4 Concentration contours for flow past an inviscid non-spherical bubble

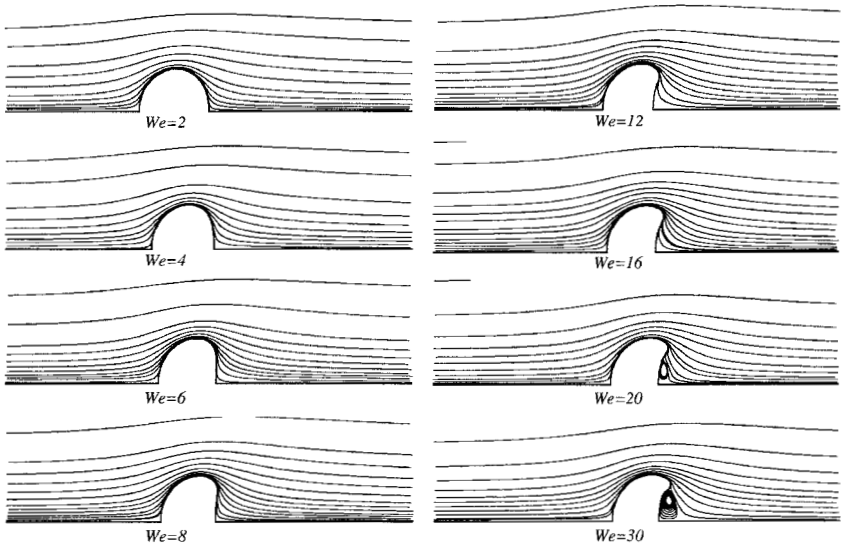

Figure 5: Evolution of bubble shape and streamlines with Weber number at Re=5

With the zonal boundary uniqueness theory and applying the novel calculating procedure of incorporating multi-block iteration and moving mesh

Paper from: *Advanced Computational Methods in Heat Transfer*, B Sunden and CA Brebbia (Editors).
ISBN 1-85312-906-2

introduced in [10], a liquid drop moving in an immiscible unbounded quiescent fluid has been simulated. Figure 6 shows the streamlines inside and outside the liquid drop for two cases. It is interesting to note that two types of returning flow have been simulated. For Case 1, a water drop falling in air with viscosity ratio (water/air) of 55, density ratio of 790 and at external Re=100, as no "break-up" of internal flow can be identified, the vortex is therefore a fluid vortex. However, for Case 2, a liquid drop moving in an immiscible unbounded quiescent fluid with viscosity ratio (internal/external) of 5, density ratio of 0.1, and at external Re=300, it can be seen that two pairs of vortices (one pair with a larger size and the other with a smaller size near the rear stagnant point) exist inside the drop. This means that, for Case 2, a "break-up" has taken place for the internal circulation of the drop and therefore the wake flow of the drop is in the form of a solid vortex. The two types of wake vortex have been extensively discussed in [10].

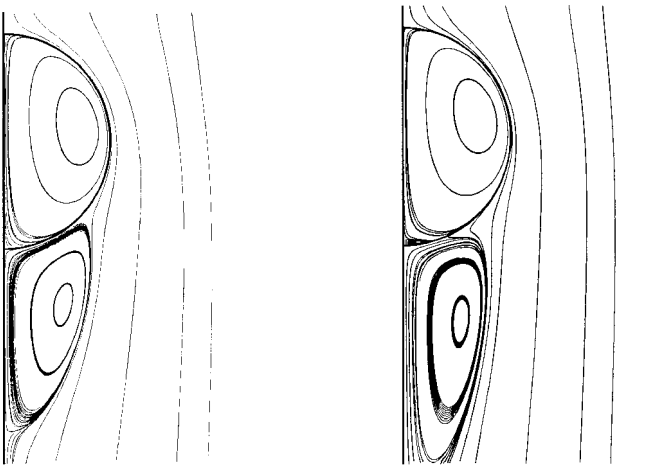

(a) Case 1 – a fluid vortex (b) Case 2 – a solid vortex

Figure 6. Flow structure inside and around a spherical droplet

4 Conclusion

This paper has summarised the authors' recent research progress on numerical modelling of transport phenomena in the vicinity of gas-liquid interface. The numerical method developed at the Nottingham Trent University can deal with slip-boundary conditions of the gas-liquid free surface and successfully simulate the terminal shape of a bubble and then the transport phenomena in the vicinity of the interface. With a zonal boundary uniqueness theory, the transport phenomena on both sides of the interface can be successfully simulated.

Paper from: *Advanced Computational Methods in Heat Transfer*, B Sunden and CA Brebbia (Editors).
ISBN 1-85312-906-2

Nomenclature

C	concentration [kg m^{-3}]
d_e	equivalent diameter [m]
J	Jacobian transformation number
Re	Reynolds number ($=\rho V_\infty d_e/\mu$)
S	source term in the general governing equation
T	temperature [K]
u	Cartesian velocity component in x-direction [m s^{-1}]
v	Cartesian velocity component in r-direction [m s^{-1}]
U, V	contravariant velocity components
V_b	Volume of a bubble [m^3]
We	Weber number ($=\rho U_\infty U_\infty d_e/\sigma$)
x, r	axisymmetric coordinate
α, β, γ	covariant metric tensors
μ	dynamic viscosity [kg m^{-1} s^{-1}]
σ	surface tension coefficient [Nm^{-1}]
τ	shear stress
ξ, η	coordinates in computational space

References

[1] Plesset, M.S. and Zwick, S.A.The growth of vapour bubble in superheated liquids, J. of Applied Physics, Vol. 25, 4, pp. 293-500, 1953.

[2] Sangani, A. S. and Didwania, A. K., Dispersed-phase stress tensor in flows of bubbly liquids at large Reynolds numbers, J. *of Fluid Mechanics,* 248, 27-54, 1993.

[3] Duineveld, P. C., The rise velocity and shape of bubbles in pure water at high Reynolds number, *Journal of Fluid Mechanics,* 292, pp 325-332, 1995.

[4] Bhaga, D. and Weber, M.E., In-line interaction of a pair of bubbles in a viscous liquid, *Chem.Eng.Sci.*35, pp. 2467-2474, 1980.

[5] Harper, J. F., Axisymmetric Stokes flow images in spherical surfaces with applications to rising bubbles. *J. Austral. Math.* Soc. B25, 217-231, 1983.

[6] Takagi, S. and Matsumoto, Y., Force acting on a rising bubble in a quiescent liquid, *ASME Conference*, Volume 1, FED-Vol. 236, pp 575-580, 1996.

[7] Takagi, S., Matsumoto, Y. and Huang, H., Numerical analysis of a single rising bubble using boundary-fitted coordinate system, *JSME International Journal, Series B*, Vol. 40, No. 1, pp 42-50, 1997.

[8] Li, W.Z. and Yan, Y.Y. An alternating dependent variables (ADV) method for treating slip-boundary conditions of free interfacial flows with heat and mass transfer, Int. J. Numerical Heat Transfer, Part B: vol. 41, 2002 (in printing).

[9] Li, W.Z. and Yan, Y.Y., A direct-predictor method for solving terminal shape of a gas bubble rising through a quiescent liquid, submitted to Int. J. of Numerical Heat Transfer, 2001.

[10] Yan, Y.Y., Lai, H., Gentle, C.R. and Smith, J.M., Numerical analysis of fluid flows inside and around a liquid drop using an incorporation of multi-block iteration and moving mesh, Presented in 7UK NCHT, Sept., 2001 and to be published in IChemE Transaction A, Chemical Engineering Research & Design, 2002.

[11] Yan, Y.Y., and Li, W.Z., Numerical investigations of the flow and heat and mass transfer at the surface of a spherical gas bubble, to be published in Int. J. Transport Phenomena, 2002.